Zn-(BDC) and Zn-(BDC)-NH 2 MOFs: Novel Photocatalysts for Desulfurization of Dibenzothiophene from Fuels

Dawud Mohammadzadeh
Urmia University
Seyed Ali Hosseini (a.hosseini@urmia.ac.ir)
Urmia University

Research Article

Keywords: Zinc metal-organic framework, Amine modified MOF, Dibenzothiophene, photocatalyst, desulfurization

Posted Date: May 9th, 2022

DOI: https://doi.org/10.21203/rs.3.rs-1564962/v1

Abstract

The paper reports the development of nanostructures of organic-metallic frameworks (MOFs) in the form of Zn(BDC) and Zn(BDC)-NH_2 as potent macroporous photocatalysts for desulfurization of aromatic hydrocarbons (dibenzothiophene) in fuels. The reason for placing amine groups in the Zn-MOF photocatalytic structure was that it increased the interaction between MOF and sulfur compounds. The experiments were designed out by the Box-Behnken method of response surface methodology (RSM) and the process was modelled and optimized. Three independent parameters i.e. concentration of dibenzothiophene, the amount of photocatalyst and light emission time were considered in the experimental design. The interactions between the parameters were also investigated by 2D contour and 3D plots. The optimum removal of DBT (50.40%) resulted under a fuel model containing 50 ppm DBT, desulfurized by 0.060 g of Zn-MOF-NH_2 photocatalyst under visible lamp light for 180 min. The predicted response (DBT removal%) by the RSM model was 50.68%. The amine-modified Zn-MOF exhibited a greater activity in the elimination of DBT due to its active amine groups. The mechanism of photocatalytic desulfurization of DBT over Zn-MOF-NH_2 was proposed. The physical-chemical properties of the MOF samples were further recognized by Fourier Transform Infrared (FTIR), X-ray diffraction (XRD), Brunauer-Emmett-Teller (BET), Field-Emission Scanning Electron Microscopy (FESEM) and Uv-Vis diffuse reflectance spectroscopy (UV-Vis DRS). This study showed that Zn-MOF can be an effective photocatalyst for desulfurization under the visible light of a fuel model.

1. Introduction

The increase in demand for fossil fuels has several reasons, including the development of industry and population growth. Sulfur compounds in fossil fuels, even in trace amounts, have created many concerns and limitations in the field of human health and the environment.

Therefore, scientists are trying to come up with very efficient methods to reduce the contaminants associated with sulfur compounds in fuels to very low levels.

Common sulfur compounds in fuels are dibenzothiophene (DBT) and its derivatives. One of the methods currently used for gasoline desulfurization is hydrocarbon desulfurization (HDS), which is used to remove sulfur compounds from hydrocarbons in oil refineries. This method is carried out under difficult conditions and also requires increasing the residence time of the reactor (Su and Hong 2004, Masoumi and Hosseini 2020). A common method used in industry for the desulfurization of liquid fuels is hydrodesulfurization. Removal of ring sulfur compounds such as dibenzothiophene (DBT) and other similar compounds can be done under difficult conditions. Recently, various methods such as extraction and oxidation of adsorption have been replaced to remove sulfur compounds such as dibenzothiophene, which require mild conditions (Jafarinasab, Akbari et al. 2020). One energy source that is very important in our lives is crude oil. However, crude oil contains various sulfur compounds that produce sulfur oxides such as SO_2 and SO_3 after burning, causing many problems such as air pollution and the environment.

To reduce the adverse effects of sulfur compounds on human health and the environment, desulfurization of petroleum slices is essential.

Metallic-organic frameworks (MOFs) photocatalysts are a new example of high porosity materials that are widely used in various fields due to their multifaceted structure, high controllable porosity, and significant surface area. Recently, the applications of energy stored in MOF-based materials have been studied in research fields. In this study, examples of recent advances in the use of MOF-based materials, such as the storage of solar energy, hydrogen, and gaseous fuels, as well as the conversion of different types of energy into each other are mentioned. Thus, advanced energy technologies with MOF-based materials were challenged and discussed (Li, Yang et al. 2020). Several materials in the class of metal-organic frameworks (MOF) were investigated to determine their sorption characteristics for sulfur compounds from fuels. The materials were tested using different model oils and common fuels such as low-sulfur gasoline or diesel fuel at room temperature and ambient pressure. Thiophenes were chosen as the model of S-containing aromatic hydrocarbons (Achmann, Hagen et al. 2010). Catalysts of organic-metallic frameworks with different organic ligands such as (NH_2-BDC, BDC, and NDC), as well as metal center structures (M, MM, and M3O), and metal ions (Zn, Cu, and Fe) to study their effects on It was used on various sulfur compounds. Experiments show that MOFs with coordinated unsaturated sites (CUS) have the strongest bonds with sulfur compounds. MOFs are second only to NH_2-BDC substituent group ligands, followed by saturated metal centers, and organic ligands without substituent groups have the weakest adsorption capacity. The results also show that among different types of metal ions (copper, zinc and iron), MOF with unsaturated iron metal (Fe-MOF) has a higher adsorption power compared to other metal ions for sulfur compounds. These results are consistent with our experimental results, and thus provide insight into the better design of the organic-metal framework catalyst for use in photo desulfurization (Chen, Ling et al. 2016).

The most recent development of MOFs as precursors for the preparation of various nanostructures and their potential applications in energy-related devices and processes. Specifically, this present survey intends to push the boundaries and covers the literature from the year 2013 to early 2017, on supercapacitors, lithium-ion batteries, electrocatalysts, photocatalysts, gas sensing, water treatment, solar cells, and carbon dioxide capture. Finally, an outlook in terms of future challenges and potential prospects for industrial applications are also discussed. (Yap, Fow et al. 2017, Akbarzadeh, Motaghi et al. 2020).

According to the literature review, so far Zn-MOFs have not been used as photocatalyst in Desulfurization. In this work, Zn-(BDC) and Zn-(BDC)-NH_2 MOFs were used as nano photocatalysts to desulfurize DBT from the fuel model. The experiments were designed by response surface methodology (RSM) and the process was modelled and optimized. The photocatalysts were characterized by X-ray diffraction (XRD), Fourier transforms infrared (FT-IR), Field emission scanning electron microscopes (FESEM), UV-visible DRS, and BET.

2. Materials And Methods

2.1. Materials

Normal heptane solvent was used in the preparation of dibenzothiophene (DBT) solution with different concentrations. Dimethylformamide (DMF) was used as a solvent to prepare the Zn-MOF photocatalyst. Ethyl alcohol was used to remove impurities from the photocatalyst.

All materials used in this research are provided by the German company Merck

2.2. Synthesis of Zinc Metal-Organic Frameworks (Zn-MOF)

The Zn-MOF photocatalyst was synthesized by the co-precipitation method described in the synthesis method:

in the synthesis method, the stoichiometric ratio of Zn(NO3)2.4H2O and the terephthalic acid was 1: 1. Thus, 0.01 mol of terephthalic acid and 0.01 mol of Zn (NO3)2.4H2O were dissolved in 40 mL of dimethylformamide solvent and mixed for 20 min.

Then an aqueous solution consisting of 2.61 g of Zn $(NO_3)_2$. $4H_2O$ (0.01mol) and 1.66g of terephthalic acid (0.01mol) are added dropwise to the solution under stirring.

After complete pouring, the solution was exposed to ultrasonic waves at room temperature for 30 minutes. The Zn-MOF photocatalyst was dried and synthesized in a 100 ° C oven for 48 hours.

2.3. Characterization of Zn-MOF photocatalyst

XRD analysis of Zn-MOF photocatalyst samples was performed using a Phillips device (PW1730). The details of this device include the size of the screening stage with a magnitude of 0.05 degrees.

Information on Fourier transform infrared (FT-IR) was obtained using a Nexus 670 spectrophotometer. To measure the energy band distance of the sample (induction band and valence band), diffuse reflectance analysis was used by a Lambda 19 UV / VIS / NIR spectrophotometer (PerkinElmer).

To determine the surface area of the samples, BELSORP MINI II (Japan) was used.

Bruker spectroscopy (TENSOR27 model) was used to analyze the FTIR of MOF nanoparticles. First, the photocatalytic and potassium bromide (KBr) nanoparticles were combined and compressed into tablets.

High-resolution images of the samples were obtained by field emission scanning electron microscopy (FESEM) (Sigma ZEISS Microscopy).

2.4. Experimental tests and experimental design

The response surface methodology (RSM) was used to design experimental tests in the phot - desulfurization process to avoid wasting time and reduce costs and better study the process model.

The performance of the Zn-MOF photocatalyst to remove DBT from the fuel sample was evaluated as follows:

According to the tests designed by Box-Benken design, the fuel model with a certain concentration of di-benzothiophene (20–80 ppm) and a definite amount of Zn-MOF photocatalyst (0.02–0.06 g) for 25 minutes at a temperature of 25°C and a pressure of 1 atmosphere under visible light inside a reactor made of Quartz was placed. The atmosphere was shaken by a magnet.

Before visible irradiation with a 250 W tungsten lamp, the suspension was stirred in a non-light (dark) medium by a magnet for 20 minutes to balance the adsorption-desorption of DBT and photocatalysts.

DBT concentration was measured by UV-VIS spectrophotometer at 300 nm (λ_{max} = 300 nm). At a wavelength of 300 nm, strong absorption indicates an n-π * stimulation similar to that for sulfur atoms in DBT.

The concentration of DBT in the fuel after photocatalytic reactions were calculated by calibration curve (Hosseini, Majidi et al. 2018).

3. Result And Discussion

3.1. Characterization of the Zn-MOF

XRD pattern was used for characterization of the structure and crystallinity of the samples and the related patterns are shown in Fig. 1. The peaks at 9.8, 15.5, 16.8 and 20.8 indicated the miller facet of (220), (400), (420), and (531), respectively. These peaks approve the MOF structure of Zn(BDC) and the pattern of NH_2-modified-Zn(DBC) did not differ so much. The lack of some crystal faces indicates that the morphology of Zn (BDC) MOF is a random slab of a certain thickness rather than a cubic crystal.

Figure 2 displays the FTIR spectra of the prepared zinc metal complex in the range of 400–4000 cm^{-1}. In Figure, the zinc–metal complex showed an absorption frequency of 3430 cm^{-1} which confirms the presence of the hydroxyl group in the complex. Peaks appearing at 2987 cm^{-1} indicate C–H stretching present in the aromatic ring and 1612 cm^{-1} were assigned due to the linker and C = O stretching lower than those of terephthalic acid, respectively which confirmed the coordination of Zn metal. The absorption band at 1544 cm^{-1} and 1502 cm^{-1} confirmed the aromatic C = C bending vibrations. Asymmetric and symmetric stretching vibrations of − COO − are appeared at 1388 cm^{-1}. The absorptions at 927 cm^{-1}, 792 cm^{-1} and 648 cm^{-1} were due to the presence of a small amount of DMF as residual solvent. The absorption peaks at 522 and 591 cm^{-1} correspond to Zn–O stretching, approving the structure of the metal coordination bond in MOF. The absence of a peak at 1700 cm^{-1} implies the removal of the carboxyl group of terephthalic acid during the reaction. The FTIR spectrum of Zn(BDC)-NH_2 (not presented) was similar to that of Zn(BDC) sample, just the peak of region 3200–3400 cm^{-1} was broader due to overlapping of NH2 and O-H peaks.

Figure 1

Figure 2

The results of SEM of the synthesized Zn-MOF are shown in Fig. 3. Due to different multiple coordination modes in the Zn-MOF crystals, multiple structures have been formed.

Figure 3

The bandgap of the synthesized MOF was calculated at 1.93 eV based on the E = 1243/λ. The calculated band gap is in agreement with the literature(Tiwari, Sagara et al. 2019). The MOF showed a lower bandgap compared to the $NiCo_2O_4$ (2.7 eV) and layered double hydroxides(Hosseini, Majidi et al. 2018, Masoumi and Hosseini 2020, Nazari and Hosseini 2021)

The chemical-physical properties of the synthesized sample are presented in Table 1. The BET surface of the photocatalyst was 19.04 $m^2.g^{-1}$ followed by isotherm type II, indicating a microporous MOF.

Table 1
The physical-chemical properties of the Zn(BDC) MOF-NH_2

Sample name	BET surface area ($m^2.g^{-1}$)	C value in BET formula	Pore volume($m^3.g^{-1}$)	Pore mean diameter (nm)
Zn(BDC)-MOF-NH_2	19.04	4.82	4.37	4.13

Table 1

3.2. Mechanism of photocatalytic desulfurization

Figure 4. shows the proposed mechanism for photocatalytic degradation of DBT over MOFs. The propulsion of the process of photo-desulfurization using Zn-MOF photocatalyst is the presence of hydroxyl radicals. The photocatalytic mechanism following the degradation of DBT at the Zn-MOF level is described. Experiments were also performed in the absence of the photocatalyst. Experiments performed in the absence of photocatalysts showed that dibenzothiophene showed high stability under visible light without Zn-MOF photocatalysts and was not degraded. The result is in agreement with the literature(Zarrabi, Entezari et al. 2015).

As mentioned above, the promoting factor for the desulfurization reaction in the presence of photocatalyst is based on the formation of radicals, especially hydroxyl radicals. The hydrogen peroxide (0.1mL) was used as a hydroxyl radical source.

During degradation of one-mole hydrogen peroxide in the presence of light on the photocatalyst, 2 mol of hydroxyl radical is produced. As a result, a chemical reaction occurs between the active hydroxyl radicals and the dibenzothiophene molecules. First, the oxidation process of the sulfur heteroatom in DBT is

carried out by a hydroxyl radical. Hydroxyl radicals attack the sulfur atom of DBT, thus breaking the covalent bond between the carbon atom and the sulfur in the dibenzo-thiophene molecule.

At the end of the reaction, sulfur is released as SO_2 gas and the biphenyl molecule is the product of this reaction.

The reason for proposing the mechanism for this process is that no trace of sulfur and its compounds remains after the end of the reaction and no compound was observed on the surface of the Zn-MOF catalyst by FTIR analysis in which sulfur atoms are presented (Zarrabi, Entezari et al. 2015).

Figure 4

3.3. Modelling and optimization of the process

As mentioned in the experimental section, the photocatalytic removal of DBT over MOF catalysts was studied by RSM and it was modelled and optimized.

The range of effective parameters in the reaction was as follows: the reaction time range was 60–180 minutes, the amount of Zn-MOF photocatalyst was 0.02–0.06 g and the concentration of dibenzothiophene was 20–80 ppm.

A total of 15 experiments were designed by the Box-Behnken method considering three levels for each parameter (-1, 0, + 1). The equation created to respond to the process is as follows:

Response = 57.0–0.315 iradiation time(min) – 8.85 photocatalyst(g) – 0.207 C(ppm) + 0.000618 iradiation time(min)*irradiation time(min) – 0.275 photocatalyst(g)*photocatalyst(g) – 0.00431 C(ppm)*C(ppm) + 0.0569 iradiation time(min)*photocatalyst(g) + 0.001667 iradiation time(min)*C(ppm) + 0.1271 photocatalyst(g)*C(ppm) (1)

The model (Eq. 1) indicates the effect of the independent parameters and the interaction of the parameters with the response. The coefficient of determination between the predicted responses and the experimental responses by the model is 97.2, which indicates that the model fits the data well.

Also, two-dimensional contour diagrams and three-dimensional surface diagrams examined and presented the interaction between the parameters (time, amount of photocatalyst, and concentration of dibenzothiophene). Figure 5 shows the two-dimensional contour and three-dimensional surface diagrams of the amount of Zn- MOF photocatalyst (gram) and the reaction time (minutes) on the desulfurization efficiency. It is deduced from Fig. 5 that the optimal response is when the reaction time is 165–180 minutes and the amount of nano photocatalyst is about 0.055–0.060 g.

Also in the two-dimensional and three-dimensional diagrams of Fig. 6, the interaction between the concentration of dibenzothiophene and the Zn- MOF photocatalyst on the response was investigated. The results of the graphs showed that the system response is most effective from the concentration of di-benzothiophene 50–75 ppm and the photocatalyst term with the value of 0.05–0.060 g. In general,

hydroxyl radicals have a rapid action in the degradation of dibenzothiophene molecules due to the high number of active centers present at the photocatalytic surface.

At higher than optimal values, the rate of degradation is low and a limited number of photocatalysts can be activated due to the increased transparency of the suspension, which increases light scattering and reduces the penetration depth of light photons.

Also, at high concentrations of dibenzothiophene, the number of active photocatalytic sites decreases due to nanoparticle occupation (Seshadri, Chitra et al. 2008, Zhang, Wu et al. 2008). Increasing the initial concentration of dibenzothiophene reduces the efficiency of the photocatalytic reaction for two reasons:

First, at high concentrations of dibenzothiophene, more of its molecules are adsorbed on the photocatalyst surface and its active sites.

Second, the number of visible light photons that reach the photocatalyst level at high concentrations of di-benzothiophene decreases, and the catalyst loses its activity significantly due to the occupation of its sites by di-benzothiophene molecules. (Mai, Lu et al. 2008, Sobana, Selvam et al. 2008)

An optimal value was then determined for the amount of Zn-MOF photocatalyst and the concentration of dibenzothiophene.

Two-dimensional and three-dimensional diagrams of Fig. 7 show the correlation between the concentration of benzothiophene and irradiation time on the response and show that the concentration of dibenzothiophene is in the range of 50–75 ppm and reaction time is in the range of 165–180 minutes has maximum value.

The optimal removal conditions of dibenzothiophene from the fuel model (gasoline) on the Zn-MOF photocatalyst were predicted by the model, which occurs in the concentration of dibenzothiophene, the amount of photocatalyst, and the reaction time of 50 ppm, 0.06 g and 180 minutes, respectively. According to the above conditions, the predicted removal efficiency of DBT was 50.68%, while the experimental experiment resulted in a removal efficiency of 50.41% of dibenzothiophene from the fuel model.

Figure 5

Figure 6

Figure 7

Conclusions

Zn-(BDC) MOF and Zn-(BDC) MOF-NH_2 were synthesized and used as novel photocatalysts for the desulfurization of dibenzothiophene from the fuel model. The results confirmed the superior activity of Zn-(BDC) MOF-NH_2. The process was modelled and optimized. The optimum removal of DBT was

50.40% and the predicted value by the RSM model was 50.68%. The optimum conditions in the study were under a fuel model containing 50 ppm DBT, photocatalyst dosage of 0.060 g of Zn-MOF-NH_2 photocatalyst under visible lamp light for 180 min. A mechanism for the oxidation of DBT over Zn-MOF-NH2 photocatalyst was developed. The bandgap of MOF indicated that the MOF could show superior activity under UV irradiation. It is concluded that Zn-MOFs could be a potent photocatalyst for fuel treatment.

Declarations

Acknowledgements

The authors especially thank the Research Deputy of Urmia University for encouraging support.

Disclosure statement

No potential conflict of interest was reported by the authors.

Funding

This work was financially supported by Urmia University.

Author Contribution:

"Dawud Mohammadzadeh as a Master's student did the experiments of his MSc thesis project and analyzed data. He wrote the original draft of the manuscript including the text, figures, and tables."

"Seyed Ali Hosseini as the supervisor guided the Mr. Mohammadzadeh project and validated the results. He edited the manuscript. All authors reviewed the manuscript. Seyed Ali Hosseini, as the corresponding author submitted it to the journal"

References

1. S. Achmann, G. Hagen, M. Hämmerle, I.M. Malkowsky, C. Kiener, R. Moos, Sulfur removal from low-sulfur gasoline and diesel fuel by metal-organic frameworks. Chem. Eng. Technology: Industrial Chemistry-Plant Equipment-Process Engineering-Biotechnology **33**(2), 275–280 (2010)
2. F. Akbarzadeh, M. Motaghi, N.P.S. Chauhan, G. Sargazi, A novel synthesis of new antibacterial nanostructures based on Zn-MOF compound: design, characterization and a high performance application. Heliyon **6**(1), e03231 (2020)
3. Z. Chen, L. Ling, B. Wang, H. Fan, J. Shangguan, J. Mi, "Adsorptive desulfurization with metal-organic frameworks: A density functional theory investigation.". Appl. Surf. Sci. **387**, 483–490 (2016)
4. S.A. Hosseini, V. Majidi, A. Abbasian, Photocatalytic desulfurization of dibenzothiophene by NiCo2O4 nanospinel obtained by an oxidative precipitation process modeling and optimization. J. Sulfur

Chem. **39**(2), 119–129 (2018)

5. M. Jafarinasab, A. Akbari, M. Omidkhah, M. Shakeri, An efficient Co-based metal–organic framework nanocrystal (Co-ZIF-67) for adsorptive desulfurization of dibenzothiophene: Impact of the preparation approach on structure tuning. Energy & Fuels **34**(10), 12779–12791 (2020)
6. X. Li, X. Yang, H. Xue, H. Pang, Q. Xu, Metal–organic frameworks as a platform for clean energy applications. EnergyChem **2**, 100027 (2020)
7. F. Mai, C. Lu, C. Wu, C. Huang, J. Chen, C. Chen, "Mechanisms of photocatalytic degradation of Victoria Blue R using nano-TiO2.". Sep. Purif. Technol. **62**(2), 423–436 (2008)
8. S. Masoumi, S.A. Hosseini, Desulfurization of di-benzothiophene from gasoil model using Ni-Co2, Ni-Fe2 and Co-Fe2 nano layered-double hydroxides as photocatalysts under visible light. Fuel **277**, 118137 (2020)
9. M. Nazari, S.A. Hosseini, Mixed oxides derived from layered double hydroxides of Ni and Co as photocatalysts for desulfurization of dibenzothiophene. J. Chem. Sci. **133**(1), 1–11 (2021)
10. H. Seshadri, S. Chitra, K. Paramasivan, P. Sinha, "Photocatalytic Degrad. liquid waste containing EDTA " Desalin. **232**(1–3), 139–144 (2008)
11. N. Sobana, K. Selvam, M. Swaminathan, Optimization of photocatalytic degradation conditions of Direct Red 23 using nano-Ag doped TiO2. Sep. Purif. Technol. **62**(3), 648–653 (2008)
12. C. Su, B. Hong, "a TSENG, C.-M." Sol–gel preparation and photocatalysis of titanium dioxide. Catal. Today **96**, 119–126 (2004)
13. A. Tiwari, P.S. Sagara, V. Varma, J.K. Randhawa (2019). "Bimetallic metal organic frameworks as magnetically separable heterogeneous catalysts and photocatalytic dye degradation." ChemPlusChem 84(1): 136–141
14. M.H. Yap, K.L. Fow, G.Z. Chen, Synthesis and applications of MOF-derived porous nanostructures. Green. Energy & Environment **2**(3), 218–245 (2017)
15. M. Zarrabi, M.H. Entezari, E.K. Goharshadi, "Photocatalytic oxidative desulfurization of dibenzothiophene by C/TiO 2@ MCM-41 nanoparticles under visible light and mild conditions. " Rsc Advances **5**(44), 34652–34662 (2015)
16. X. Zhang, F. Wu, X. Wu, P. Chen, N. Deng, Photodegradation of acetaminophen in TiO2 suspended solution. J. Hazard. Mater. **157**(2–3), 300–307 (2008)

Figures

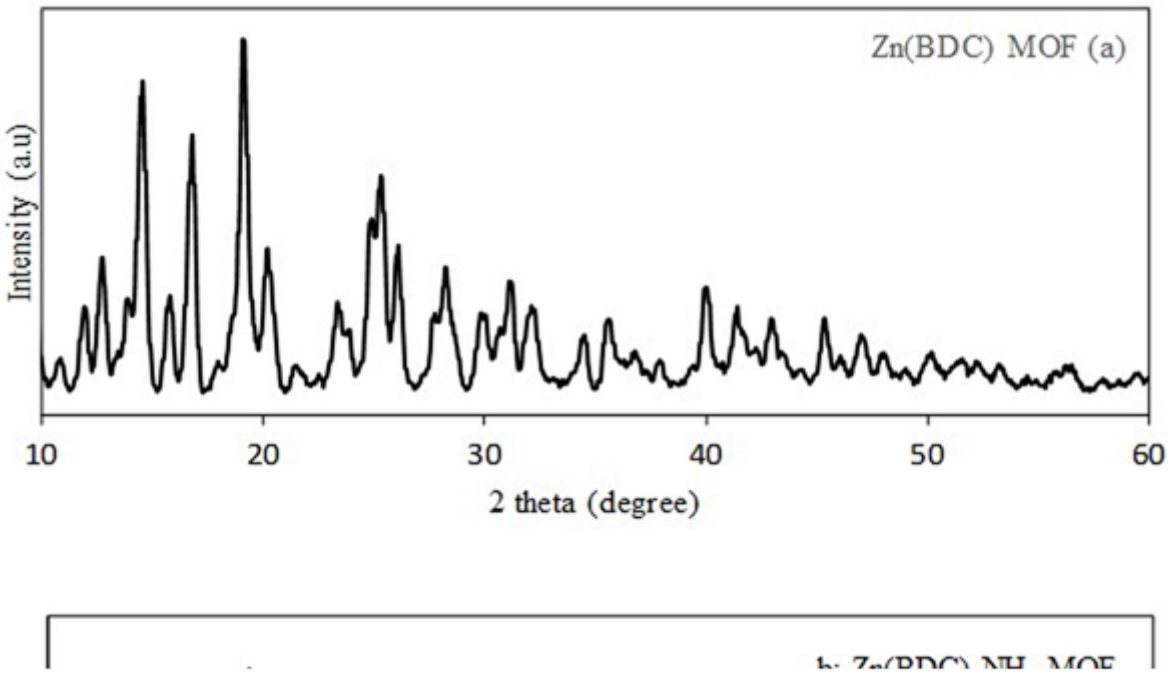

Figure 1

XRD pattern of Zn(BDC) (a) and NH_2-modified Zn(BDC) (b)

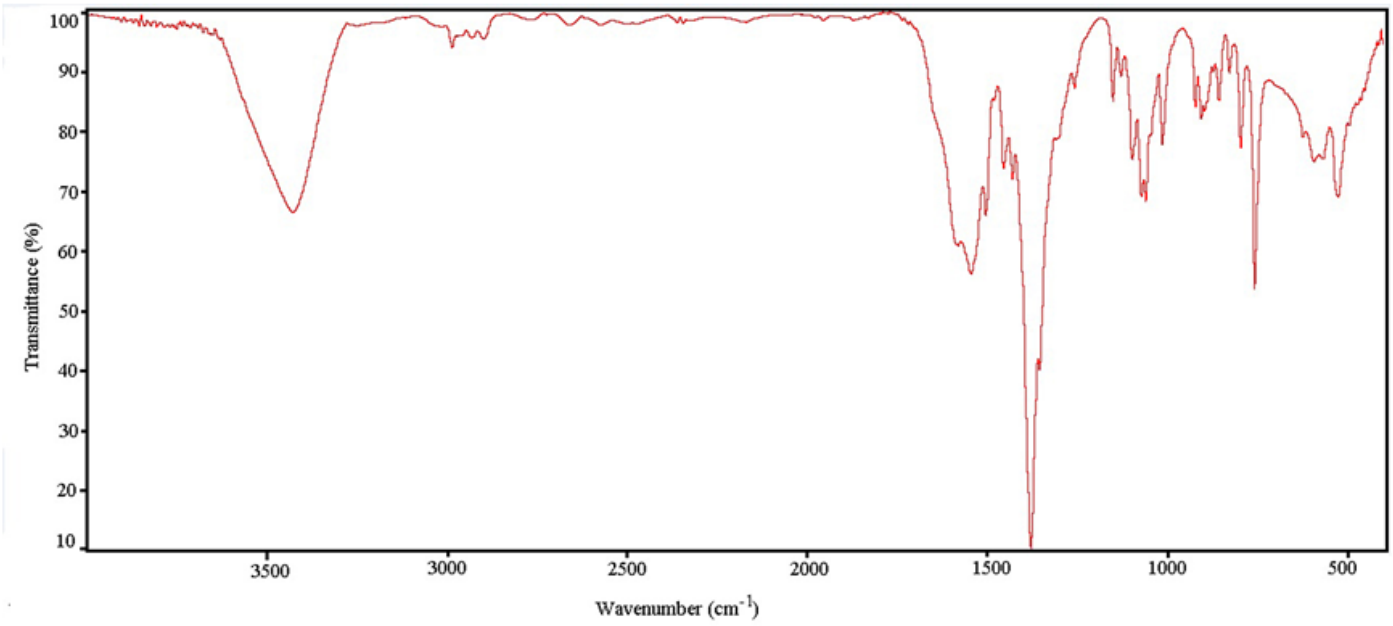

Figure 2

FTIR spectrum of Zn(BDC) MOF

Figure 3

SEM images of the synthesized MOFs. Zn(BDC) (a) and Zn(BDC)-NH_2 (b).

Figure 4

Mechanism of photocatalytic desulfurization of DBT over Zn-(BDC) MOF

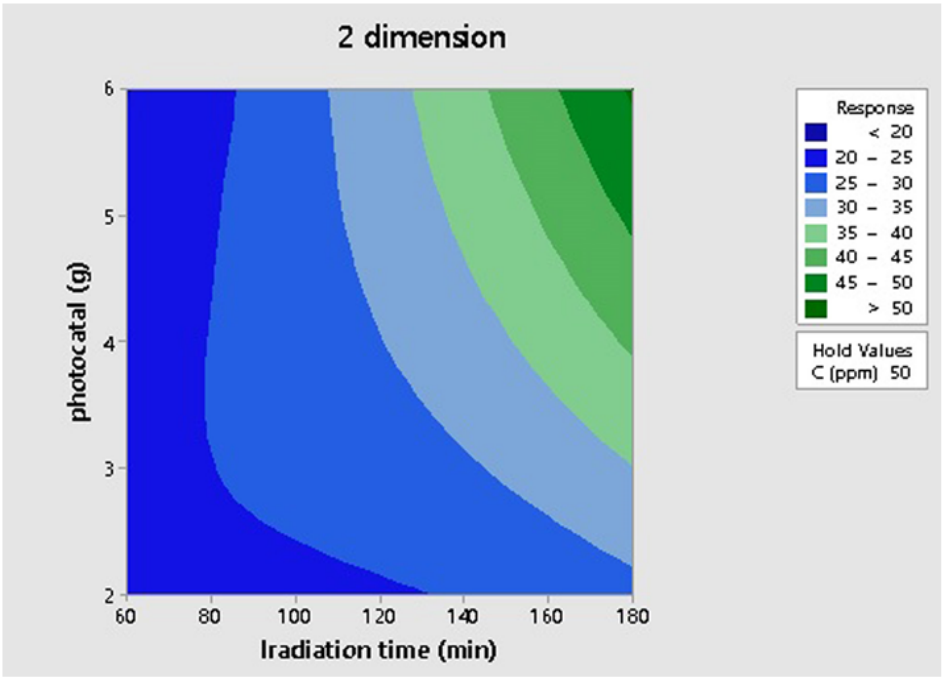

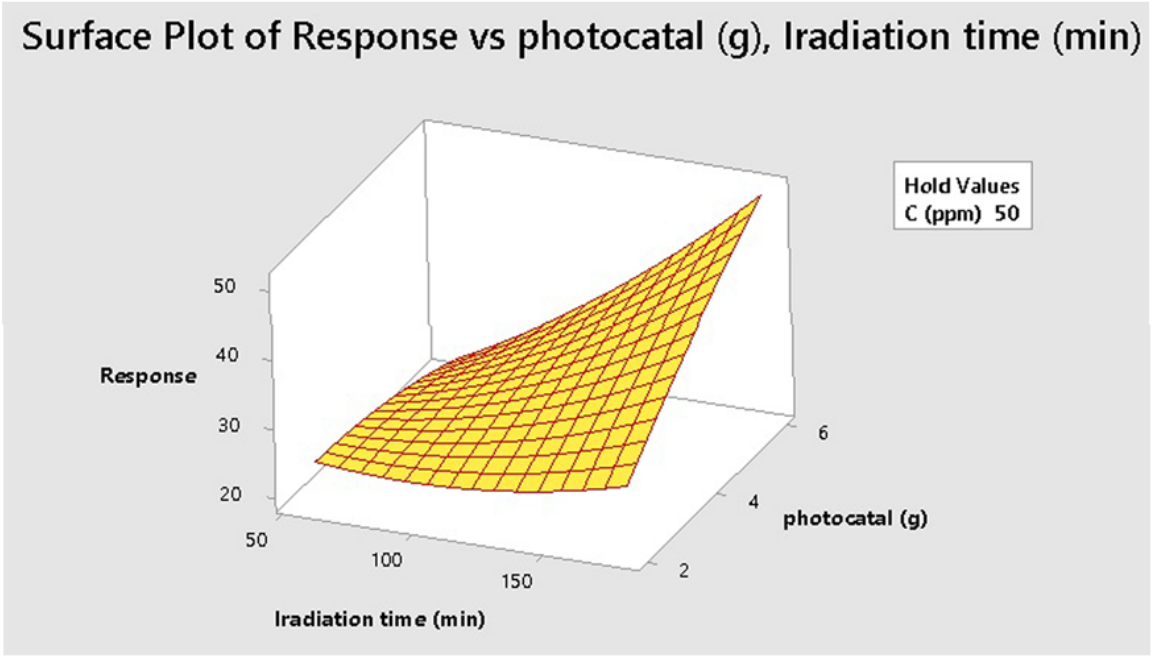

Figure 5

Contour plot and Surface plot of Response vs photocatalyst and Irradiation time

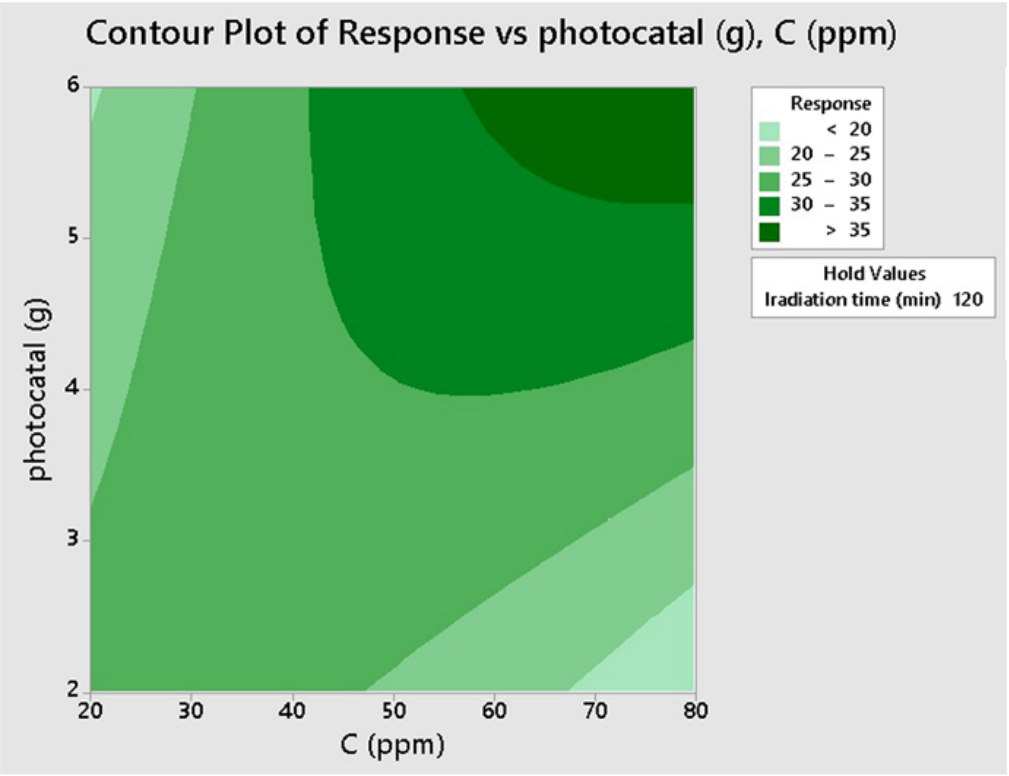

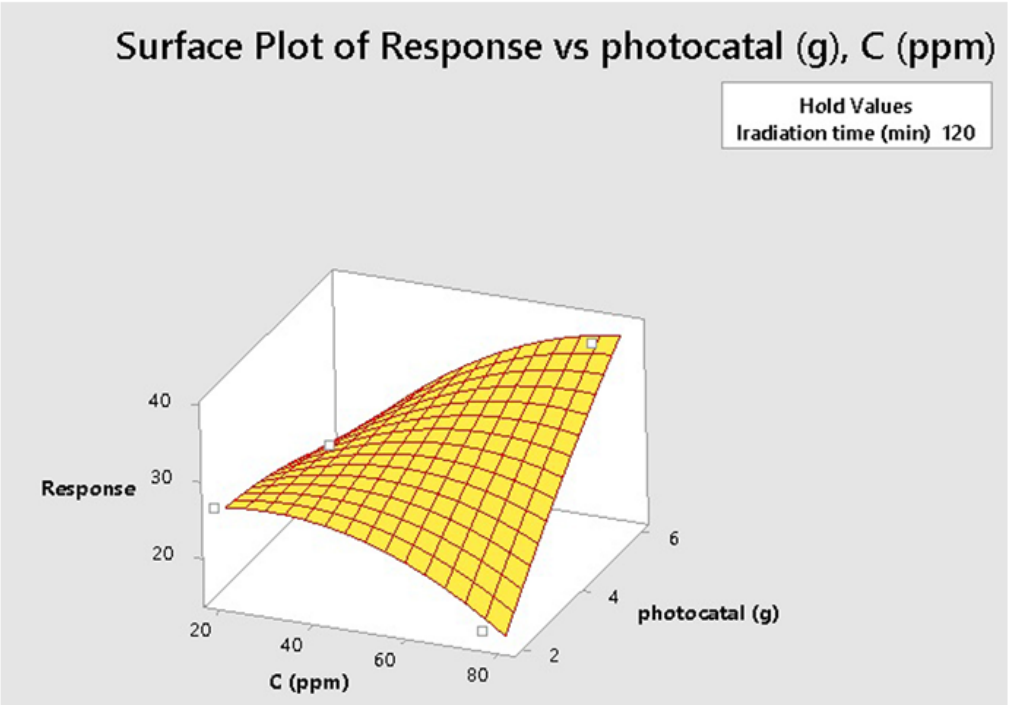

Figure 6

Contour plot and Surface plot of Response vs photocatalyst dosage and DBT Concentration

Figure 7

Contour plot and Surface plot of Response vs Irradiation time and DBT Concentration